City Research Online

City, University of London Institutional Repository

Citation: Mascio, A. A., Roman, A. J., Cideciyan, A. V., Sheplock, R., Wu, V., Garafalo, A. V., Sumaroka, A., Pirkle, S., Kohl, S., Wissinger, B., et al (2023). Color Vision in Blue Cone Monochromacy: Outcome Measures for a Clinical Trial. Translational Vision Science & Technology, 12(1), 25. doi: 10.1167/tvst.12.1.25

This is the published version of the paper.

This version of the publication may differ from the final published version.

Permanent repository link: https://openaccess.city.ac.uk/id/eprint/29916/

Link to published version: https://doi.org/10.1167/tvst.12.1.25

Copyright: City Research Online aims to make research outputs of City, University of London available to a wider audience. Copyright and Moral Rights remain with the author(s) and/or copyright holders. URLs from City Research Online may be freely distributed and linked to.

Reuse: Copies of full items can be used for personal research or study, educational, or not-for-profit purposes without prior permission or charge. Provided that the authors, title and full bibliographic details are credited, a hyperlink and/or URL is given for the original metadata page and the content is not changed in any way.

City Research Online: http://openaccess.city.ac.uk/ publications@city.ac.uk

tvst

Retina

Color Vision in Blue Cone Monochromacy: Outcome Measures for a Clinical Trial

Abraham A. Mascio[1], Alejandro J. Roman[1], Artur V. Cideciyan[1], Rebecca Sheplock[1], Vivian Wu[1], Alexandra V. Garafalo[1], Alexander Sumaroka[1], Sydney Pirkle[1], Susanne Kohl[2], Bernd Wissinger[2], Samuel G. Jacobson[1], and John L. Barbur[3]

[1] Scheie Eye Institute, Department of Ophthalmology, Perelman School of Medicine University of Pennsylvania, Philadelphia, PA, USA
[2] Molecular Genetics Laboratory, Institute for Ophthalmic Research, Centre for Ophthalmology, University of Tuebingen, Tuebingen, Germany
[3] Centre for Applied Vision Research, School of Health Sciences, City, University of London, London, UK

Correspondence: Artur V. Cideciyan, Scheie Eye Institute, University of Pennsylvania, 51 N. 39th Street, Philadelphia, PA 19104, USA. e-mail: cideciya@pennmedicine.upenn.edu

Received: September 1, 2022
Accepted: December 23, 2022
Published: January 24, 2023

Keywords: clinical trial; color; cone photoreceptor; visual pigment gene mutations; outcome measure

Citation: Mascio AA, Roman AJ, Cideciyan AV, Sheplock R, Wu V, Garafalo AV, Sumaroka A, Pirkle S, Kohl S, Wissinger B, Jacobson SG, Barbur JL. Color vision in blue cone monochromacy: Outcome measures for a clinical trial. Transl Vis Sci Technol. 2023;12(1):25, https://doi.org/10.1167/tvst.12.1.25

Purpose: Blue cone monochromacy (BCM) is an X-linked retinopathy due to mutations in the *OPN1LW/OPN1MW* gene cluster. Symptoms include reduced visual acuity and disturbed color vision. We studied BCM color vision to determine outcome measures for future clinical trials.

Methods: Patients with BCM and normal-vision participants were examined with Farnsworth–Munsell (FM) arrangement tests and the Color Assessment and Diagnosis (CAD) test. A retrospective case series in 36 patients with BCM (ages 6–70) was performed with the FM D-15 test. A subset of six patients also had Roth-28 Hue and CAD tests.

Results: All patients with BCM had abnormal results for D-15, Roth-28, and CAD tests. With D-15, there was protan-deutan confusion and no bimodal tendency. Roth-28 results reinforced that finding. There was symmetry in color vision metrics between the two eyes and coherence between sessions with the arrangement tests and CAD. Severe abnormalities in red-green sensitivity with CAD were expected. Unexpected were different levels of yellow-blue results with two patterns of abnormal thresholds: moderate elevation in two younger patients and severe elevation in four patients $\geq$35 years. Coefficients of repeatability and intersession means were tabulated for all test modalities.

Conclusions: Given understanding of advantages, disadvantages, and complexities of interpretation of results, both an arrangement test and CAD should be useful monitors of color vision through a clinical trial in BCM.

Translational Relevance: Our pilot studies in BCM of arrangement and CAD tests indicated both were clinically feasible and interpretable in the context of this cone gene disease.

Introduction

With increasing progress in therapeutic approaches to previously incurable and rare inherited retinal degenerations (IRDs), there is now a need for outcome measures to determine the safety and efficacy of novel treatments. Standard outcomes that have been mainly used for clinical trials in common retinal diseases such as diabetic retinopathy and age-related macular degeneration (AMD) need to be supplemented with assays that relate to specific manifestations of the rare IRDs.[1,2] For example, an X-linked inherited retina-wide cone photoreceptor disease, blue cone monochromacy (BCM), is being considered for gene augmentation therapy.[3] A plan for a BCM gene therapy would be to deliver to the central retina, preferably by an intravitreal viral vector, a normal functional copy of the *OPN1LW/OPN1MW* gene, which in BCM has disease-causing variants.[4–6]

The clinical features of BCM have been recognized for decades, and there have been many in-depth studies of visual function in patients with BCM.[7–12] There is consensus that BCM causes a congenital visual acuity

Copyright 2023 The Authors

This work is licensed under a Creative Commons Attribution-NonCommercial-NoDerivatives 4.0 International License.

Downloaded from tvst.arvojournals.org on 03/01/2023

reduction and color vision abnormality. Most studies agree that there is loss of function of the green and red cones but retained blue cone and rod function.[4,13] There are also many reports in the literature that BCM can manifest a slowly progressive foveal-central macular degeneration.[4,13–16]

Proof-of-concept research showing cone function restoration in murine and nonhuman primate models of BCM has been performed using a gene augmentation therapeutic approach.[17–22] Considering that the main manifestations of BCM are reduced visual acuity and abnormal color vision, efficacy of any human clinical trial of a therapy should include assays of these visual functions. In addition to the conventional outcome of best-corrected visual acuity (BCVA), we recently addressed the related patient complaint of difficulty in reading and determined what parameters of reading performance could be quantified.[23]

Is there a standard color vision test for clinical trials? A survey of recent trials of achromatopsia, another retina-wide cone photoreceptor disease with visual acuity and color vision abnormalities, suggests that a battery of color vision tests rather than a single method has been more commonly used.[24–27] Previous studies of color vision in BCM have also used a variety of tests.[13,28] In the present study, we address the need for color vision testing parameters in natural history studies and in preparation for treatment trials of BCM. A pragmatic approach was used to select which tests to evaluate for feasibility in a multicenter trial. Among criteria used were availability, previously published experience in BCM or at least in clinical settings, and methods that lend themselves to quantitation of results. Given administration of therapy, there should be sufficient sensitivity of the method to detect change from baseline. Based on our previous studies of foveal structure and function,[29,30] the hypothesis entering a clinical trial of BCM is that an efficacious outcome would be an improvement in visual function and not a slowing of negative change. The timeframe for such improvement in BCM is not known, but for rod function in another recent photoreceptor-based gene therapy trial, it was determined to be within days to weeks of dosing.[31]

Two arrangement tests and the computer-based Color Assessment and Diagnosis (CAD) test were used. The arrangement tests derive from the Farnsworth–Munsell 100 Hue, which was first described more than 75 years ago.[32] The D-15 and Roth-28 arrangement tests use less hues and thereby take less time to perform.[33–37] Repeatability for the D-15 test has been reported in color-defective participants.[38] The CAD test can measure red-green (RG) and yellow-blue (YB) chromatic sensitivity using dynamic luminance contrast noise to isolate the use of color signals. RG and YB color thresholds and the severity of any loss have been measured in clinical studies of AMD, diabetes, aniridia, color vision deficiencies, and mild hypoxia, as well as in a trial of diabetic macular edema treated with intravitreal steroid implants.[39–42] Within- and intersubject variabilities for this test have been studied in normal and color-defective participants,[43] and the test also computes an approximate measure of variability of single measurements within a session. Building on a long history of scientific interest in color vision, discovery of the basis of color vision deficiencies most recently at the molecular level, and medical advances that could lead to human therapy,[44] the current studies begin to determine which assays of color vision could be useful as outcome measures for clinical trials of patients with BCM.

Methods

Human Participants

The study included 36 patients (median age, 30.3 years; range, 7–70 years) with a clinical and molecular diagnosis of BCM. Molecular testing of the patients and their families has been previously reported.[3,45,46] Twenty-one patients had large structural variants at the *OPN1LW/OPN1MW* gene cluster (i.e., large deletion mutations), and 15 patients carried the p.C203R missense mutation in single or multiple *OPN1LW/OPN1MW* genes. Procedures followed the Declaration of Helsinki, and the study was approved by the University of Pennsylvania Institutional Review Board. Informed consent was obtained from adults and assent with parental permission from children. All patients had a complete eye examination.

Experimental Procedures

Experiment 1

Farnsworth–Munsell (FM) standard D-15 panel was used in all 36 patients to determine whether there are different patterns of results within our cohort of patients with BCM. The test was carried out using standardized procedures.[37] There are 16 colored caps: 1 fixed and 15 moveable. The patient's task is to order the moveable caps so as to minimize the perceptual difference between adjacent caps, beginning with the cap judged to be the closest match to the fixed cap. Testing was performed monocularly, with refractive correction, and under lluminant C (Macbeth Lamp, X-Rite, Inc., 1000 lx, Grand Rapids, Michigan, USA). A second session for D-15 metrics was obtained after a period not exceeding 5 years from the first.

Downloaded from tvst.arvojournals.org on 03/01/2023

Experiment 2

Roth-28 Hue testing, a compromise version of the FM D-15 and 100 Hue arrangement tests, uses every third color cap from the 100 Hue (which has 85 caps). The patient is asked to arrange the moveable caps in a circular sequence starting from a fixed cap.[34] All testing was performed in a light booth (Pantone 3-D50, Color Confidence, Birmingham, UK); illuminance was 1460 lx, and calibration occurred prior to each patient session. Six patients (P10, P16, P17, P23, P31, P33) performed this test. The tests for both eyes and both sessions were performed on the same day.

Experiment 3

The CAD test is intended to quantify loss of RG and YB chromatic discrimination sensitivity.[43] The test employs a fully calibrated, 10-bit visual display, and the patient views a uniform background field of ~7° × 7° and luminance of 24 cd/m^2, which approximates daylight at ~6500K (CIE chromaticity 0.305, 0.323). The color-defined test stimulus moves diagonally across a center foreground square defined by flickering checks, which vary randomly in luminance, with equal probability within a range specified as a percentage of background luminance. The luminances of the center ~3° × 3° flickering foreground and the ~0.9° × 0.9° moving colored stimulus remain constant and equal to that of the uniform background. The use of dynamic luminance contrast noise ensures that the participant cannot make use of any residual luminance contrast signals to detect the moving colored stimulus.[47] The full test employs chromatic displacement directions defined by the background chromaticity and each of 16 points on the spectrum locus chosen to stimulate selectively either RG or YB chromatic mechanisms. This allows accurate classification of the patient's class of congenital or/and acquired deficiency. In this study, we selected only eight chromatic displacement (CD) directions, which are sufficient to quantify severity of RG and YB loss. The color signal strength along each direction was controlled by a staircase procedure according to the patient's response to each stimulus presentation. If the patient identifies correctly the direction of the moving stimulus twice during sequential presentation of the same color (i.e., up-right, up-left, lower-right, or lower-left), the algorithm reduces the chromatic saturation of the stimulus by decreasing its CD value, bringing its chromaticity closer to that of the background so as to make it more difficult to see the stimulus and hence to respond correctly during the next presentation of the same color during the test sequence. When the patient fails to produce a correct response, the CD value for the corresponding color is increased so as to make it easier to produce a correct response during the next presentation. Each staircase employs 11 reversals, and the threshold is calculated by averaging the last 6 reversals. This procedure yields the color signal strength needed to achieve a 71% correct response.[48] Within a session, the program measures separate color thresholds in eight directions. Each direction is indicated by the angle the chromatic displacement direction makes with respect to the horizontal axis. The angles selected correspond to displacement directions from the neutral background chromaticity toward the yellow (60° and 64°), green (150° and 165°), blue (240° and 244°), and red (330° and 345°) regions of the spectrum locus. The software additionally produces two normalized metrics to summarize the severity of color deficiency: the "RG" and "YB" thresholds in "standard CAD units." One CAD unit represents the mean threshold RG and YB color signal strengths measured in 330 healthy young normal trichromats.[41,49,50] Data were collected with a turnkey system (Eizo CS2420 monitor and AVOT software; City Occupational Ltd, Cumbria, UK) with parameterization appropriate for low vision,[40] viewing distance of 1.4 m and double the stimulus size employed in the normal protocol, a reduced number of directions (8 instead of 16), and a higher random noise modulation of 98%. The latter is needed to ensure that in the absence of normal cone responses, the patients cannot make use of rod-mediated luminance signals to detect the moving stimuli when highly saturated colors are employed.

Training videos to explain the CAD method using suprathreshold color signals were recorded on a tablet and presented to the patient before testing began. Testing was started only after it was clear that the patient understood the task. CAD was performed monocularly and with appropriate refractive correction. The same six patients (P10, P16, P17, P23, P31, P33) as in experiment 2 performed this test. The tests for both eyes and both sessions were performed on the same day.

Optical Coherence Tomography

Optical coherence tomography (OCT) cross-sectional images of the central retina horizontally through the fovea were obtained using SD-OCT (Optovue RT-100; Optovue Inc., Freemont, California, USA) in the same subset of six patients with BCM who also had color vision testing. The purpose was to try to relate photoreceptor structure with color-related visual function in BCM. Methods for segmentation analysis and measurement of outer nuclear layer (ONL) thickness have been described previously.[46]

Downloaded from tvst.arvojournals.org on 03/01/2023

Data Analysis

Experiments 1 and 2: FM D-15 and Roth-28 Hue

Results were quantified using the moment of inertia method.[51] This method computes the major and minor radii of gyration and confusion angle from the color difference vectors joining the color coordinates of the cap sequences as arranged by the patient. We analyzed the angle, which can be compared to those found on the three common color deficiencies; the confusion index (C-index: length of the major radius relative to normal, a normalized error score that is equal to 1 in a perfect order sequence); and the S-index (ratio of major/minor radii, indicating the degree of polarity versus randomness of the difference vectors: high values indicate strong polar orientations typical of dichromatic observers).

Experiment 3: CAD

The software produces values for the CDs for the eight directions tested and two aggregates (RG and YB thresholds). For simplicity, the CDs were pooled into four groups of similar directions (60°/64°, 150°/165°, 240°/244°, 330°/345°).

Statistical Analyses

Groupwise summary statistics were calculated. Interocular and intersession variability were quantified as the 95% interval of the differences between eyes (right (OD) minus left (OS)), or sessions (S2 minus S1), respectively, as 2.77 * SD, with SD obtained from the residual variances in a linear model. Evidence for bimodality was tested using Hartigans' test.[52] Comparison across mutations was performed by a two-sample t-test, $\alpha = 0.05$. R software (R Core Team, Vienna, Austria) was used for all analyses.

Results

Patients with BCM had Early Treatment Diabetic Retinopathy Study (ETDRS) BCVA within the range from 20/63 to 20/250 (0.5 to 1.1 logMAR); all patients had myopic refractive errors. There were 21 patients with *OPN1LW/OPN1MW* large deletion mutations and 15 with the p.C203R missense genotype (Supplementary Table S1[46]). Certain additional ocular abnormalities were detected on clinical examination that could impact the results. P1 had a unilateral macular coloboma, and data were not collected in the affected right eye. P30, P31, P32, P35, and P36 had minimal nuclear sclerosis in the lens of both eyes when examined at ages ranging from 55 to 70 years. P33, at age 64, showed 1 to 2+ minimal nuclear sclerosis in both eyes and a 1+ posterior subcapsular opacity in the right eye.

Arrangement Tests: FM D-15 and Roth-28 Hue

FM D-15

All 36 patients with BCM had abnormal D-15 results (Supplementary Table S1). For all eyes at earliest sessions, median (interquartile range [IQR]) were 5.8° (16°), 3.1 (0.9), and 2.6 (1.3) for Angle, C-index and S-index, respectively. A comparison based on mutation type showed no statistically significant differences between the means of both groups ($P = 0.5$, 0.4, and 0.6 for Angle, C-index, and S-index, respectively).

The three metrics (Angle, C-index, and S-index) for the patients with BCM are plotted (Fig. 1A). In normal subjects, a perfect sorting sequence gives an Angle of 50° as the individual color difference vectors change orientation regularly at each step, with no preferential angles resulting in low polarity. In our cohort of patients with BCM, Angle is centered near 0° and the distribution has long tails to either side (Fig. 1A, left). The C-index (severity) is far from the normal (value 1), with values widely spread across the cohort (Fig. 1A, center). The S-index (polarity) is also spread (Fig. 1A, right): a number of eyes were close to the normal value of 1.38, which indicates little polarization; the rest show higher degrees of polarization.

For the rest of the analysis, we separated the more extreme values of the Angle distribution (values lower than 1.5 * IQR and higher than 1.5 * IQR from the lower and upper quartiles, respectively). They are displayed as green and red filled circles (Figs. 1B, 1C). The relationship between Angle and C-index is shown (Fig. 1B). Blue circles represent the majority of eyes studied, without the extreme values. The median Angle in this subset was 3.7° and the distribution did not appear bimodal ($P = 0.18$, Hartigans' test); there was no clear separation into protan and deutan deficiencies (medians of 5° and −12°, respectively).[45] If a cutoff angle of −3° was used to discriminate the defect,[38] 66% of the sessions would be classified as protan-like. Sessions with higher C-index values also show higher S-index (Fig. 1C), which indicates that results become more coherent in terms of orientation of the defect when the color deficiency is more severe.

Data from selected patients were chosen to further illustrate the cap arrangement patterns with D-15 in BCM (Fig. 2). Two had high C-index values (symbols surrounded by red circles, Fig. 1B); two had low values (symbols surrounded by red squares, Fig. 1B), and there were two representative patients from both tails

Downloaded from tvst.arvojournals.org on 03/01/2023

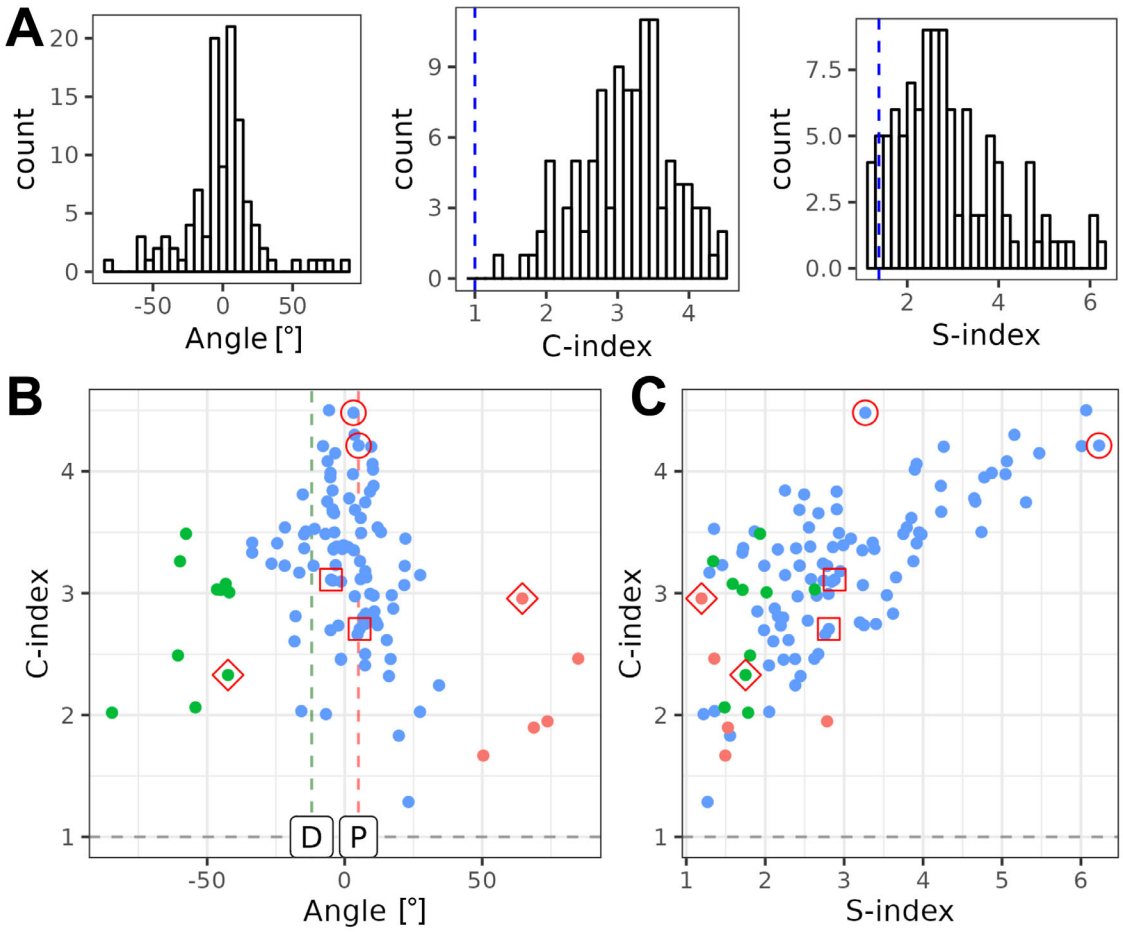

Figure 1. FM D-15 parameters in patients with BCM. (**A**) Distribution of Angle, C-index, and S-index values. Normal, *vertical blue dashed line* (in C-index and S-index). (**B**) Relation between Angle and C-index values. *Blue symbols*: data located within ±1.5 IQR from quartiles of the Angle distribution; they cluster around 0°, near the average deutan (D) and protan (P) axes. Tails of the Angle distribution are displayed as *green* and *red filled circles*. Two patients with high C-index values, two with low C-index values, and two on the upper and lower tails are marked with *red open circles*, *squares*, and *diamonds* around the *filled symbols*, respectively. Data are further illustrated in Figure 2. (**C**) Sessions showing higher C-indices (more severe dysfunction) tend to have higher degrees of polarity (coherence on the direction of errors). *Dashed horizontal lines* at ordinate 1 indicate the C-index value for normal controls.

of the angle distribution (symbols surrounded by red diamonds, Fig. 1B). P3 and P5 (Fig. 2A) with high C-index values (4.2 and 4.5, respectively) show many mistakes around a similar confusion angle. P3 shows higher polarity (more coherence across the mistake angles) than P5 (S-index values of 6.2 and 3.3). Both patients' angle parameters (5.1° and 3.2°) correspond with the protan axis (red dashed line at 5° inclination). In contrast, P12 and P16 (Fig. 2B) show less mistakes with correspondingly lower C-index values (3.1 and 2.7, respectively), and the patterns are less polar (S-index of 2.9 and 2.8, respectively). The angle parameter is closer to the deutan axis (green dashed line at −12° inclination) in P12 and to the protan axis in P16. P31 and P27 (Fig. 2C) are examples of patterns showing high or low angle parameters (tails of the distribution in Fig. 1A; left, diamonds in Fig. 1B). In both cases, the polarities are low (1.8 and 1.2, respectively), indicating that the mistakes are spread around different angles of confusion. The degrees of confusion (C-indices 2.3 and 3, respectively) are similar to the examples in Figure 2B.

Roth-28 Hue

The six patients with BCM studied with the Roth-28 test had abnormal results (Fig. 3), with varying degrees of confusion. Four patients showed a more severe pattern (Fig. 3A), with higher C-index values (5.5, 5.4, 5.2, and 4.1 for P33, P17, P31 and P23, respectively). The remaining two patients, P16 and P10, had less severe color defects with C-indices of 3.3 and 3.2 (Fig. 3B).

The polarity indices are not high in both groups but for different reasons: in the first, the many errors show inconsistent (random) directions, and in the second, the

Downloaded from tvst.arvojournals.org on 03/01/2023

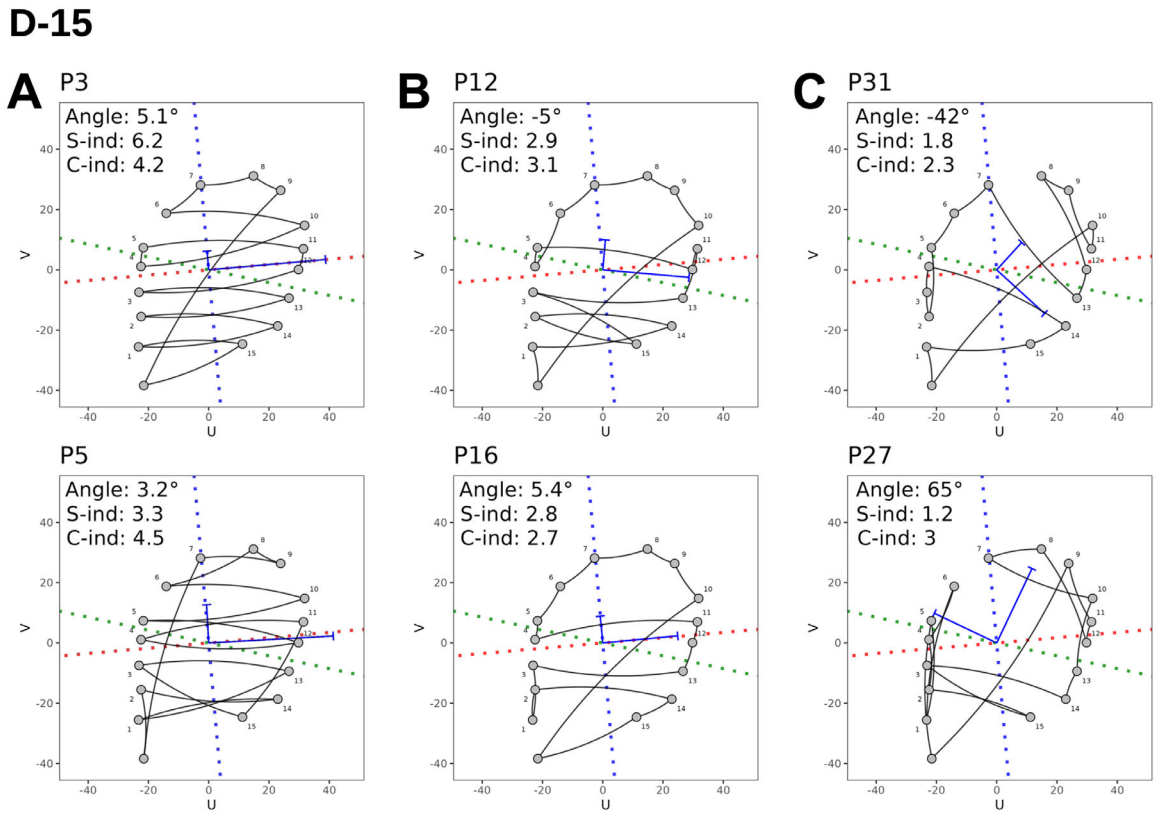

Figure 2. Representative D-15 results in BCM on CIE 1976 UV space. Cap arrangement patterns for (**A**) two patients with high C-index values (P3, top; P5, bottom) and (**B**) two patients with low C-index values (P12, top; P16, bottom). These four patients are highlighted in Figure 1B as *squares* and *circles* around *blue symbols*. (**C**) Cap arrangement patterns for two patients in the tails of the Angle distribution (P31, top; P27, bottom). All parameters are shown in the *upper-left corners*. *Bracketed blue solid lines* indicate major and minor radii of gyration. *Dashed lines*, confusion axes: protan (*red*, +5°), deutan (*green*, −12°), and tritan (*blue*, −85°).

many transitions that are error free are due to regular (not random) change of directions that happen around the normal sequence. The angle is closer to the deutan axis for patients with less severe defects (Fig. 3B). Metric values for all patients are given (Supplementary Table S2). For all eyes and sessions, median (IQR) were as follows: −38.7° (42.2°), 4.5 (1.6), and 1.7 (0.4) for Angle, C-index and S-index, respectively.

Comparison of D-15 and Roth-28 Results

The scores in patients who had both D-15 and Roth-28 tests at the same session were compared for the three parameters. A weak correlation was observed for Angle (Pearson's $\rho = 0.3$) (Fig. 3C).

CAD

The same subset of six patients with BCM was tested with the CAD method (right and left eyes tested monocularly, each twice on the same day; $n = 24$ sessions). In the CAD test result illustrations (Figs. 4A, 4B), there is a portion of the CIE 1931 x–y color space including the display limits (gray-line polygon) and the achromatic background locus at the center (black diamond). Open symbols in color represent the patient thresholds in each hue direction (counterclockwise, 60° and 64°, yellow symbols; 150° and 165°, green; 240° and 244°, blue; 330° and 345°, red). Greater distances from the center (higher CDs) indicate more severe color discrimination dysfunction in the particular direction. The ellipse in the center shows the normal upper limit (symbols outside the ellipse correspond to color departures from white that are detectable by normal controls).

Results for two representative patients (P33 and P16) show different patterns of dysfunction. P33 (Fig. 4A, pattern A) had very elevated CDs in all directions, with those for 60°/64° and 150°/165° (white to yellow and white to green directions, respectively) reaching the color rendering limits of the display device, which constitutes a floor effect in the measurements. The display limits are technically not reached in the other directions (240°/244° and 330°/345°) but remain very close to them. These results indicate almost

Downloaded from tvst.arvojournals.org on 03/01/2023

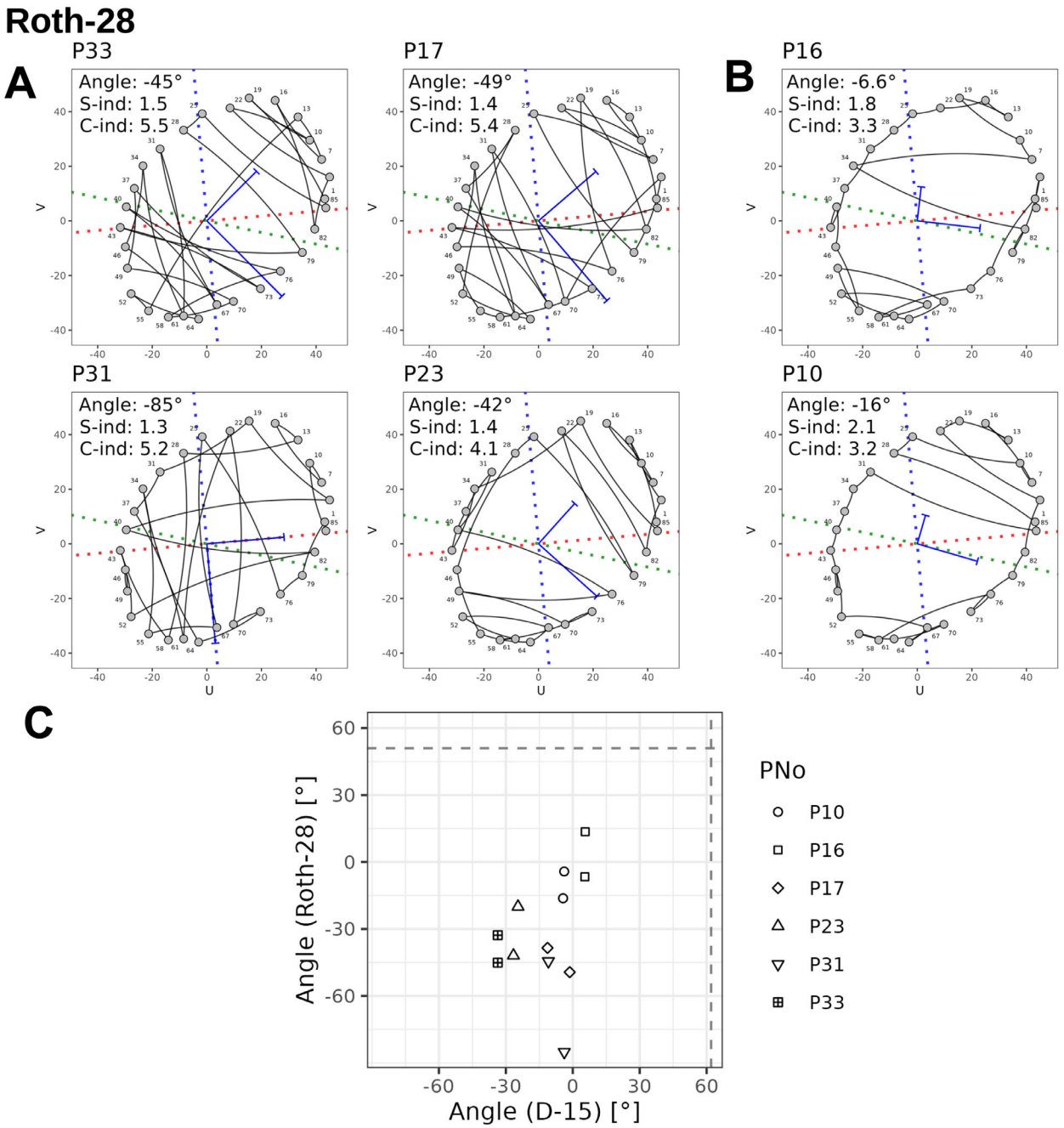

Figure 3. Roth-28 Hue arrangement patterns in BCM (first session in six patients). (**A**) Patients showing a pattern with higher dysfunction. (**B**) Patients with a pattern showing milder dysfunction. (**C**) Relationship between D-15 and Roth-28 results for the Angle parameter; *dashed lines*: angles for perfect arrangement. Other plotting characteristics and annotations as in Figure 2.

complete absence of both RG and YB chromatic sensitivity. P16 (Fig. 4B, pattern B) exhibits similar absence of RG color vision (i.e., 150°/165° and 330°/345° directions) but significant, residual YB chromatic sensitivity with YB thresholds outside the expected normal limits. The only moderately elevated CDs in the YB directions in P16 (60°/64° and 240°/244°, white to yellow and to blue, respectively) imply clear ability to discriminate color differences along the tritan axis. Both patterns show symmetry across eyes (horizontally adjacent panels) and reproducible results on both testing sessions (vertically). Data for all patients tested are plotted (Fig. 4C), showing the range of CD results observed for the cohort along all eight directions tested. The normalized summary metrics provided by the test (RG and YB thresholds) are shown (Fig. 4D). RG

translational vision science & technology

Downloaded from tvst.arvojournals.org on 03/01/2023

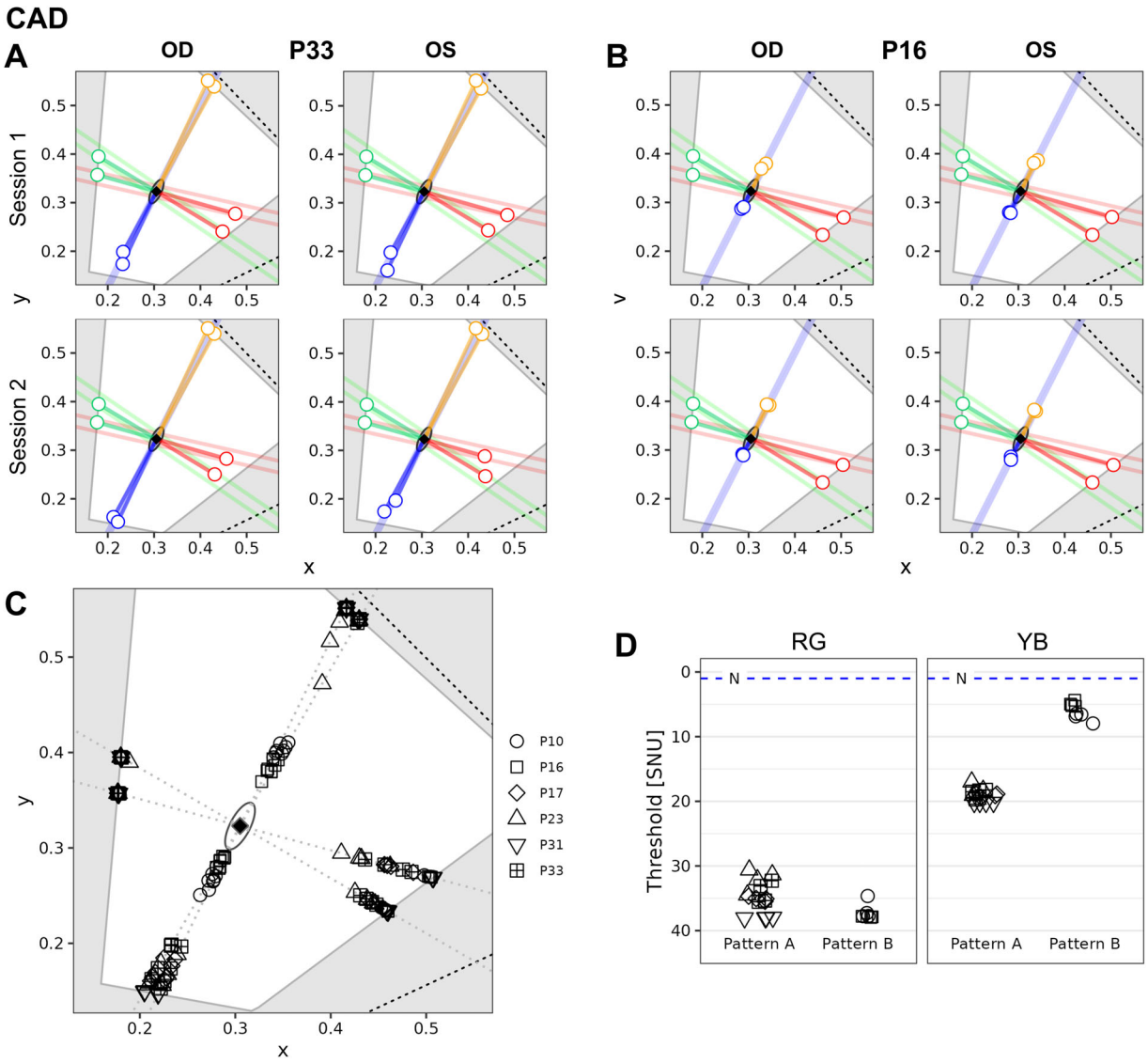

Figure 4. CAD results in BCM. (A, B) Thresholds obtained for two representative patients shown on the CIE 1931 x–y plane. *Diamond*, chromaticity coordinates for the achromatic background; *ellipse* delimits the discrimination ability in normal controls, who can detect chromaticities located outside it. *Gray-delimited white polygon*: color-rendering capability ("phosphor limits") of the device. *Open circles* indicate the patient color thresholds for each of the eight directions tested; their distance to the *diamond* indicates severity of dysfunction in the respective direction. Dimmer *red*, *green*, and *blue solid lines* delimit confusion loci for protan, deutan, and tritan deficiencies, respectively. All data tested in each patient (both eyes, horizontally and two sessions, vertically) are shown. (**A**) Patient (P33) showing severe discrimination defects in all directions. (**B**) Patient (P16) showing severe defects in the RG directions but with milder deficiency on the YB directions. (**C**) CAD data for the complete cohort. (**D**) Summary CAD RG and YB thresholds for the cohort. All patients show elevated R–G thresholds, close or at the display limits (left). This is also seen for YB in some patients (pattern A) but not in others (pattern B) that show milder deficiencies in this axis. Ordinates are in CAD Standard Normalized Units (SNU), with 1 corresponding to normal mean (N, *blue line*). Note that the SNU dynamic range for YB thresholds is smaller than for RG because of the higher variability of normal controls in that direction. The pattern A patients' thresholds are close to or at the display limits (floor effect) near 20 SNU.

thresholds were highly elevated in all patients, indistinct across patterns; in contrast, the YB threshold clearly showed the two-pattern dichotomy.

CAD results are tabulated for individual patients at both sessions (Supplementary Table S3). CAD metrics distribution parameters are given in Supplementary Table S4, separately for patients showing patterns A and B. Across patterns (vertically in the table), medians are similar for RG axis-related metrics (150°/165°, 330°/345°, RG) but differ significantly for those YB axis related (60°/64°, 240°/244°, YB).

Downloaded from tvst.arvojournals.org on 03/01/2023

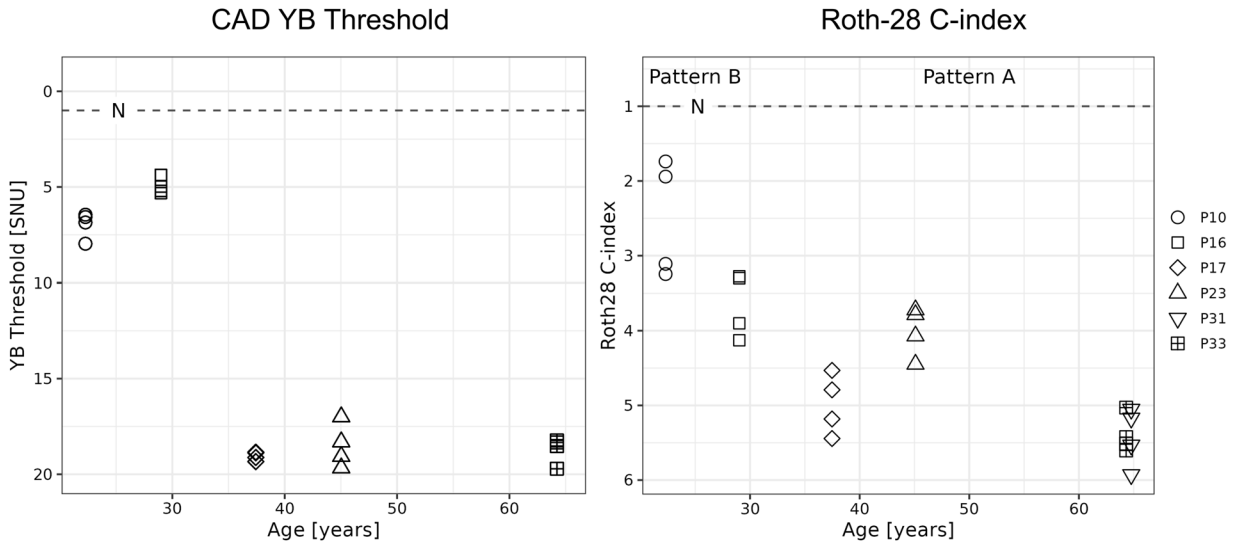

Figure 5. Relationship of color deficiencies to age. Older patients show higher dysfunction in the Y–B axes and higher confusion indices in the Roth-28 test. N, normal.

Color Dysfunction and Age

The observation of different levels of loss of YB chromatic sensitivity in the whole cohort leading to the pattern A and B classification prompted us to look at the relationship of this parameter with age (Fig. 5, left). Only cross-sectional data are available, but younger patients show the B-pattern with only moderate elevation of YB thresholds, and all patients ≥35 years of age showed the A-pattern, with severely elevated thresholds close to the instrumentation floor effect. Dependency of severity with age is also present on the Roth-28 tests results (Fig. 5, right).

Interocular and Intersession Variability

With some exceptions, there was symmetry in color vision metrics between the two eyes using the

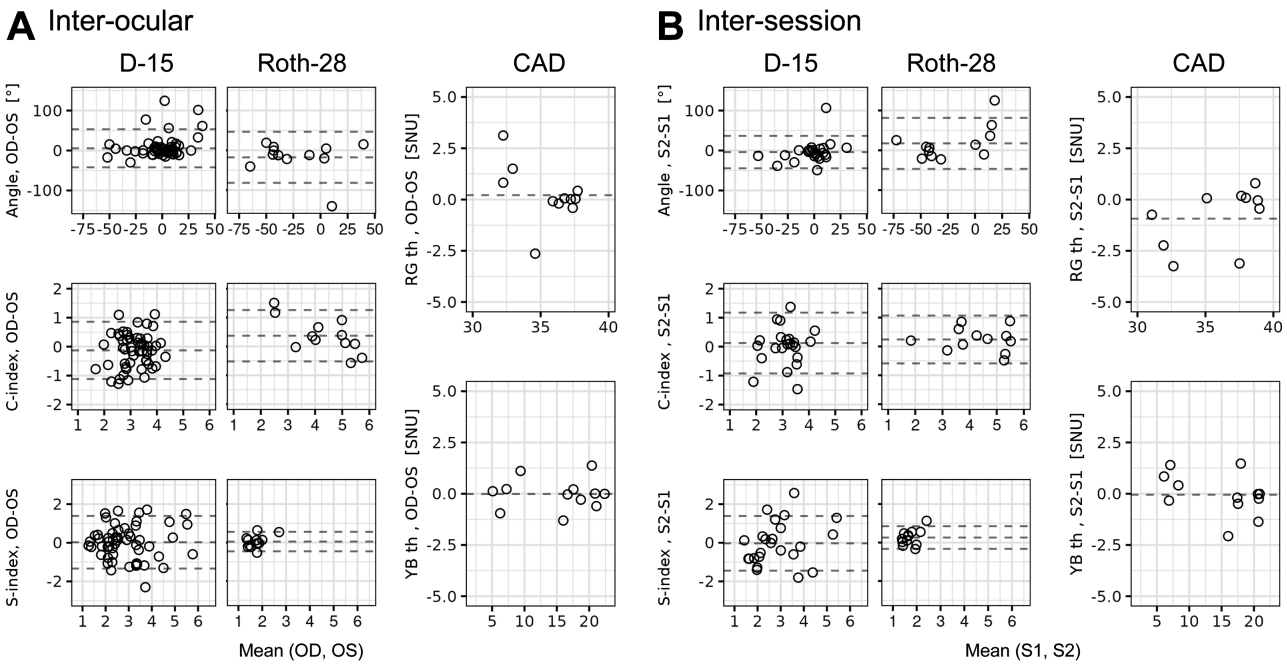

Figure 6. Color vision variability in patients with BCM using D-15, Roth-28, and CAD testing. Ordinates are OD minus OS for interocular differences (**A**), and session 2 (S2) minus session 1 (S1) for intersession differences (**B**). *Dashed lines* at mean and 95% limits for the respective differences. Data for CAD test (not censored for floor effects) also plotted for reference.

translational vision science & technology

Downloaded from tvst.arvojournals.org on 03/01/2023

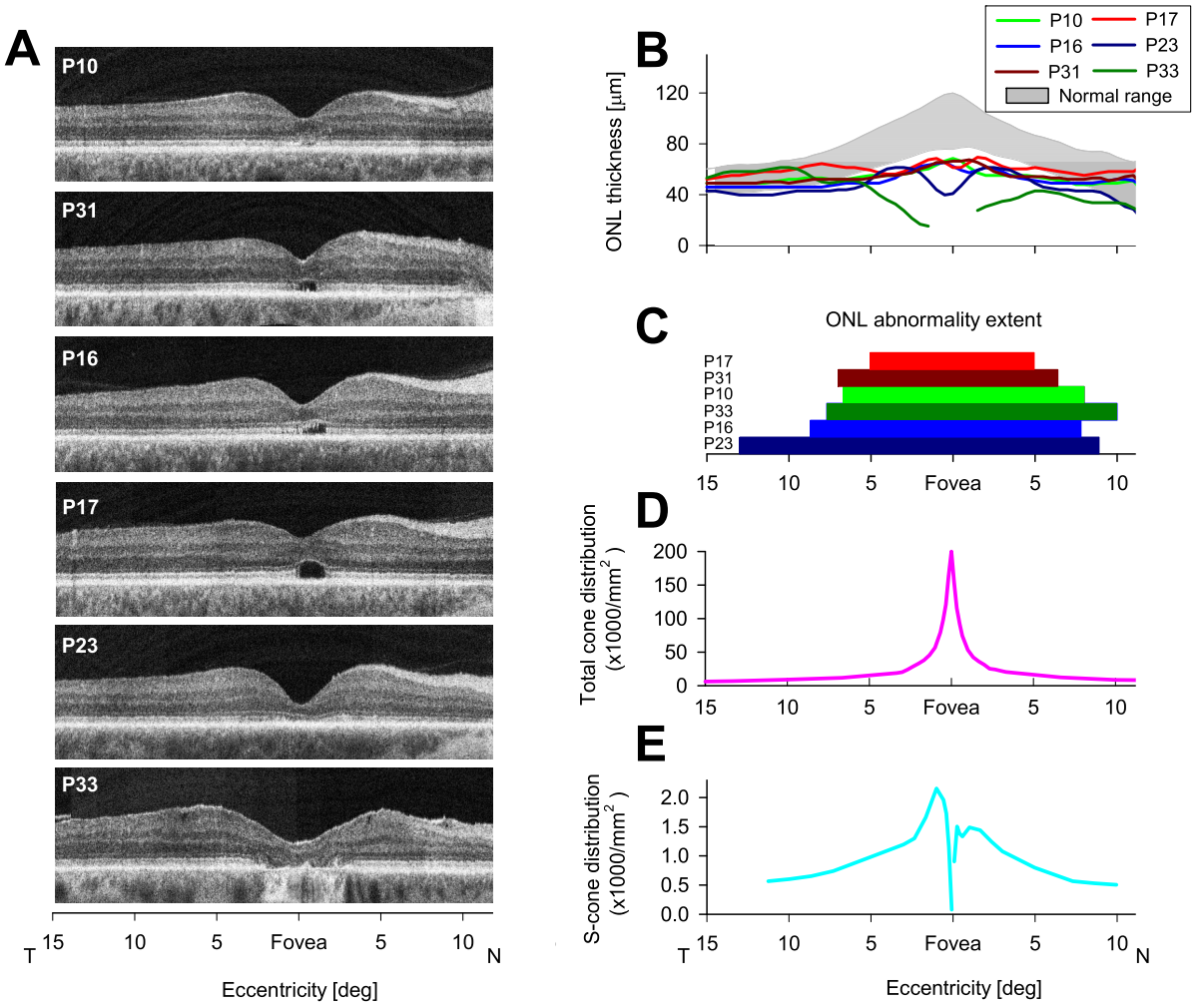

Figure 7. BCM retinal structure and cone distribution. (**A**) Central OCT scans across the horizontal meridian and through the fovea of the 6 patients with BCM studied with CAD and Roth-28 tests. The scans are ordered by foveal ONL thickness. (**B**) ONL thickness profile across the horizontal meridian of the patients (colors relate to individual patient data) compared with normal range (*gray shaded area*). (**C**) Extent of the ONL abnormality for each patient. (**D**) Distribution of total cones and (**E**) S-cones across the horizontal profiles (adapted from Curcio et al.[53,54]). N, nasal retina; T, temporal.

two arrangement tests and the CAD (Fig. 6A), as well as coherence between sessions (Fig. 6B). Data are tabulated (Supplementary Table S5). The CAD software provides standard errors (SEs) for the CDs in each direction, an indication of the variability observed within the session. In most cases, these reported SEs remain within 0 to 0.01 (median, 0.0011). Since these SEs are based on variability within the last six reversals of the staircase, they are less informative when the thresholds reach the limits imposed by the visual display. CAD intersession variability could not be assessed in the presence of floor effects. Variability from the limited YB data available from two patients (not affected by floor effects) was in agreement with previous reports.[43]

Central Retinal Structure Abnormalities in BCM

We studied with OCT the six patients with BCM with CAD scores to determine if there were any notable differences between central retinal structure in the group versus normal; comparisons were also made between individuals within the patient group (Fig. 7). These patients all had reduced central retinal ONL but of differing extents. These photoreceptor

translational vision science & technology

Downloaded from tvst.arvojournals.org on 03/01/2023

structural abnormalities spanned the central retinal area that included the normal peak density region for total cones and for blue cones.[53,54] The two patients (P10 and P16) with lowest YB thresholds, albeit abnormal, could be interpreted as having less central ONL thickness reduction. The two older patients with BCM (P31, P33) also had modest nuclear sclerosis lens changes, although there has been discussion that such changes may not be sufficient to alter YB function.[13,55] The retinal structural evidence with OCT supports the earlier clinical observations that BCM is not a stationary congenital defect in red–green cone pigments but can be complicated by a component of progressive central retinal degeneration.[13–16]

Discussion

Given the need for an outcome measure of color vision in future clinical trials of BCM, we examined two arrangement tests and one computer-based test, CAD. The three methods were feasible to perform in a clinical setting and produced quantifiable results. In general, the FM arrangement tests are more quickly performed than the CAD test. Physical limitations of the CAD color display occasionally resulted in floor effects for certain parameters in patients with the most severe abnormalities. It is encouraging, however, that there is published experience with all of these methods in other retinopathies.[33–42]

The FM D-15 can provide information about the type and severity of a defect in color vision.[37,56] Commonly, the test results are visually inspected and scored by the number of major crossings. The goal is usually to detect patterns of color blindness. All the patients with BCM in this study showed abnormalities. How do the color vision results in the current study compare with previous findings? Using D-15 panels, patients with BCM have been described as showing errors along the protan and deutan axes but none along a tritan axis[57,58] or showing protan-like patterns.[13] Are such findings indicative of absent RG but normal YB color vision in these patients? These kind of errors are also found in dichromats and rod monochromats arising as a result of matched excitations in rods and S-cones: when carrying out the D-15 tests, the patients can make use of both S-cone and rod signal differences to arrange the caps, and errors only occur when two caps generate similar rod and S-cone excitations.[59] Since caps with matched rod and/or S-cone signals align approximately along deutan and protan color confusion lines, it is not too surprising that patients with BCM who have S-cones and functioning rods confuse caps with similar excitations, explaining their D-15 results and therefore not necessarily implying normality of YB color vision. The absence of tritan errors can also be accounted for by the monotonic changes in S-cone signal strength and may not require the use of color signals. In the current group of patients with BCM, we quantified the results with the moment-of-inertia method, which provided data for three metrics: Angle, C-index and S-index.[51] We did not find a clear separation into protan and deutan deficiencies: our data suggest protan–deutan confusion, but there was no bimodal tendency on the Angle metric, with long tails to either side of the cutoff value. Our more limited data on Roth-28 Hue testing reinforced that finding. These results are not unexpected since they are consistent with loss of RG color vision. Symmetry in the calculated angles of the two eyes using the two arrangement tests adds support to the idea that the results are consistent within patients.

A key question to ask in anticipation of a clinical trial is whether results of an outcome measure on a visit differed from those on a subsequent or previous visit. We asked how D-15 severity of the defect in the patients with BCM compared between visits. For the usual clinical assessment of number of crossings, the difference to next visit is small in most cases (median absolute difference, 2; IQR, 1 to 3 crossings; Supplementary Table S1). If a pass/fail classification (fail with $\geq$2 crossings) was used, agreement between visits is 100% because of the severity of the disease. In the absence of any RG color signal, patients with BCM are expected to make major crossing errors that correspond to caps of approximately equal S-cone and/or rod excitations. Reductions in the number of D-15 major crossing errors would require substantial improvements in RG color vision. Using the C-index severity metric, the value at the next visit is expected to remain within $\pm$1 units of the first (Supplementary Table S5; 95% interval for the C-index difference between visits is $\pm$1.05). The number of crossings correlates strongly with the C-index in patients with BCM ($r = 0.88$), like observations in a cohort of patients with heterogeneous color deficiencies ($r = 0.99$[60]). Similar results are obtained for Roth-28 tests: in this case, the C-index intervisit difference in BCM is expected to be within $\pm$0.79 index units.

Given the arrangement test results in a cohort of untreated patients with BCM, what could be expected in a clinical trial, for example, of *OPN1LW/OPN1MW* gene augmentation therapy? Baseline Angle, C-index, and S-index results are expected to fall within the ranges determined in the BCM cohort of the present study. The severity of the initial abnormalities, however, will complicate determining if an intervention leads to reduced function (e.g., to gauge toxicity). No detectable

Downloaded from tvst.arvojournals.org on 03/01/2023

change in a result, however, would be helpful to know. As an efficacy assay, an arrangement test that shifted values toward lower levels of severity (lower C-index) could, of course, be informative. The interpretation of changes in S-index and Angle depends on the severity level and should be considered individually in this class of tests.

The CAD test results in our patients with BCM reveal highly elevated RG thresholds often limited by the gamut of the visual display, as anticipated from the absence of functioning L- and M-cones. This outcome is consistent with results from previous studies of BCM and current understanding of the underlying molecular defects. For a clinical trial of BCM, this floor effect of most RG thresholds at baseline may well represent complete absence of RG color vision, as expected in the case of rod monochromats and dichromats.[59] A sizable lowering of either RG or YB thresholds, however, should be quantifiable and indicative of color vision being present after intervention. The use of the RG threshold as a safety parameter for an intervention is limited to those cases when either the baseline assessment or the expected improvement yields thresholds lower than those imposed by the limits of the display. RG and YB thresholds that are limited only by the gamut of the visual display are indicative of complete absence of color vision in rod monochromats and also in RG dichromats who accept any red/green mixture as a match to the monochromatic yellow field in anomaloscope matches.[59] This is also likely to be the case in patients with BCM when the measured RG thresholds are limited by the gamut of the display, as observed in most patients in our cohort. CAD color thresholds that are well below the limits of the display are indicative of residual color signals for both RG and YB chromatic mechanisms. The CAD test, which is more lengthy to administer than the arrangement tests, is nevertheless very valuable as it allows assessing true color signals (the large 98% dynamic luminance contrast noise employed ensures that residual luminance contrast signals remain undetectable). The clinical ocular examination, imaging of the macula, and mesopic and photopic visual acuity assays are likely to be adequate measures of any decline in structure and function to monitor safety.

The patients with BCM we studied with CAD showed different patterns of YB thresholds, with some patients having only moderate threshold elevations and others showing severely elevated thresholds. The patterns of YB dysfunction in our small cohort seemed to be related to age of the patient. Fundamental studies of spectral sensitivity in BCM have determined that there is blue cone function in addition to rod function; whether the blue cones are functioning normally has received less attention.[13,57,61,62] Some of the descriptions of patients with BCM in families have reported age-related issues: color vision testing with a D-15 panel showed a protan–deutan pattern while older affected members had an anarchic pattern, which is usually noted in achromats.[13] Discussions have ensued about the basis of the presumed loss of S-cone function, and hypotheses about contributing factors included yellowing of lens opacities or the presence of subclinical or clinical maculopathy that can occur in BCM at later ages.[4,5,13,61]

The YB abnormalities may be considered progressive (versus stationary) color defects. Reports using CAD methods have shown YB dysfunction in patients with age-related macular degeneration and in diabetic patients.[39,41] Reduction of S-cone sensitivity with age has been noted in studies of various progressive retinal degenerations using many different methods.[63–66] Changes in YB function with age in BCM could be explained by a macular degenerative component. If it was the case that the lower YB thresholds are reflecting the output of a chromatic mechanism based on comparison of rod and S-cone signals, the residual YB chromatic sensitivity observed is likely to be affected by progressive retinal degenerations of rods and/or S-cones.

In summary, quantified arrangement tests could be of value as measures of color vision in a clinical trial of BCM, but their inability to control for residual luminance signals is a limitation. The dynamic luminance contrast noise in CAD tests permits isolation of true YB color signals and therefore makes this test an important component of the battery of outcome measures in trials for BCM.

Acknowledgments

Supported by Adverum Biotechnologies, Inc., the BCM Families Foundation, and unrestricted funds from Research to Prevent Blindness.

Disclosure: **A.A. Mascio**, None; **A.J. Roman**, None; **A.V. Cideciyan**, None; **R. Sheplock**, None; **V. Wu**, None; **A.V. Garafalo**, None; **A. Sumaroka**, None; **S. Pirkle**, None; **S. Kohl**, None; **B. Wissinger**, None; **S.G. Jacobson**, None; **J.L. Barbur**, (CAD test inventor), City Occupational Ltd. (E)

References

1. Csaky KG, Richman EA, Ferris FL. Report from the NEI/FDA ophthalmic clinical trial design and endpoints symposium. *Invest Ophthalmol Vis Sci*. 2008;49(2):479–489.

Downloaded from tvst.arvojournals.org on 03/01/2023

2. Csaky K, Ferris F, Chew EY, Nair P, Cheetham JK, Duncan JL. Report from the NEI/FDA endpoints workshop on age-related macular degeneration and inherited retinal diseases. *Invest Ophthalmol Vis Sci*. 2017;58(9):3456–3463.
3. Cideciyan AV, Hufnagel RB, Carroll J, et al. Human cone visual pigment deletions spare sufficient photoreceptors to warrant gene therapy. *Hum Gene Ther*. 2013;24(12):993–1006.
4. Nathans J, Davenport CM, Maumenee IH, et al. Molecular genetics of human blue cone monochromacy. *Science*. 1989;245(4920):831–838.
5. Nathans J, Maumenee IH, Zrenner E, et al. Genetic heterogeneity among blue-cone monochromats. *Am J Hum Genet*. 1993;53:987–1000.
6. Wissinger B, Baumann B, Buena-Atienza E, et al. The landscape of submicroscopic structural variants at the *OPN1LW*/*OPN1MW* gene cluster on Xq28 underlying blue cone monochromacy. *Proc Natl Acad Sci USA*. 2022;119(27):e2115538119.
7. Blackwell H, Blackwell O. Rod and cone receptor mechanisms in typical and atypical congenital achromatopsia. *Vis Res*. 1961;1(1–2):62–107.
8. Alpern M, Lee GB, Spivey BE. π1 cone monochromatism. *Arch Ophthalmol*. 1965;74(3):334–337.
9. Daw NW, Enoch JM. Contrast sensitivity, Westheimer function and Stiles-Crawford effect in a blue cone monochromat. *Vision Res*. 1973;13(9):1669–1680.
10. Young RS, Price J. Wavelength discrimination deteriorates with illumination in blue cone monochromats. *Invest Ophthalmol Vis Sci*. 1985;26(11):1543–1549.
11. Hess RF, Mullen KT, Zrenner E. Human photopic vision with only short wavelength cones: postreceptoral properties. *J Physiol*. 1989;417:151–172.
12. Reitner A, Sharpe LT, Zrenner E. Is colour vision possible with only rods and blue-sensitive cones? *Nature*. 1991;352(6338):798–800.
13. Michaelides M, Johnson S, Simunovic MP, et al. Blue cone monochromatism: a phenotype and genotype assessment with evidence of progressive loss of cone function in older individuals. *Eye (Lond)*. 2005;19:2–10.
14. Ayyagari R, Kakuk LE, Coats CL, et al. Bilateral macular atrophy in blue cone monochromacy (BCM) with loss of the locus control region (LCR) and part of the red pigment gene. *Mol Vis*. 1999;5:13.
15. Weleber RG. Infantile and childhood retinal blindness: a molecular perspective (The Franceschetti Lecture). *Ophthalmic Genet*. 2002;23(2):71–97.
16. Kellner U, Wissinger B, Tippmann S, Kohl S, Kraus H, Foerster MH. Blue cone monochromatism: clinical findings in patients with mutations in the red/green opsin gene cluster. *Graefes Arch Clin Exp Ophthalmol*. 2004;242(9):729–735.
17. Mancuso K, Hauswirth WW, Li Q, et al. Gene therapy for red-green colour blindness in adult primates. *Nature*. 2009;461(7265):784–787.
18. Zhang Y, Deng WT, Du W, et al. Gene-based therapy in a mouse model of blue cone monochromacy [published corrections appears in *Sci Rep*. 2018;8(1):4807]. *Sci Rep*. 2017;7(1):6690.
19. Deng WT, Li J, Zhu P, et al. Human L- and M-opsins restore M-cone function in a mouse model for human blue cone monochromacy. *Mol Vis*. 2018;24:17–28.
20. Deng WT, Li J, Zhu P, et al. Rescue of M-cone function in aged Opn1mw–/– mice, a model for late-stage blue cone monochromacy. *Invest Ophthalmol Vis Sci*. 2019;60(10):3644–3651.
21. Zhu P, Dyka F, Ma X, et al. Disease mechanisms of X-linked cone dystrophy caused by missense mutations in the red and green cone opsins. *FASEB J*. 2021;35(10):e21927.
22. Ma X, Sechrest ER, Fajardo D, et al. Gene therapy in *Opn1mw–/–*/*Opn1sw–/–* mice and implications for blue cone monochromacy patients with deletion mutations. *Hum Gene Ther*. 2022;33(13–14):708–718.
23. Semenov EP, Sheplock R, Roman AJ, et al. Reading performance in blue cone monochromacy: defining an outcome measure for a clinical trial. *Trans Vis Sci Tech*. 2020;9(13):13.
24. Zein WM, Jeffrey BG, Wiley HE, et al. *CNGB3*-achromatopsia clinical trial with CNTF: diminished rod pathway responses with no evidence of improvement in cone function. *Invest Ophthalmol Vis Sci*. 2014;55(10):6301–6308.
25. Zobor D, Werner A, Stanzial FB, et al. The clinical phenotype of *CNGA3*-related achromatopsia: pretreatment characterization in preparation of a gene replacement therapy trial. *Invest Ophthalmol Vis Sci*. 2017;58(2):821–832.
26. Kahle NA, Peters T, Zobor D, et al. Development of methodology and study protocol: safety and efficacy of a single subretinal injection of rAAV.hCNGA3 in patients with CNGA3-linked achromatopsia investigated in an exploratory dose-escalation trial. *Hum Gene Ther Clin Dev*. 2018;29(3):121–131.
27. Fischer MD, Michalakis S, Wilhelm B, et al. Safety and vision outcomes of subretinal gene therapy targeting cone photoreceptors in achromatopsia: a nonrandomized controlled trial. *JAMA Ophthalmol*. 2020;138(6):643–651.

Downloaded from tvst.arvojournals.org on 03/01/2023

28. Gardner JC, Liew G, Quan YH, et al. Three different cone opsin gene array mutational mechanisms with genotype-phenotype correlation and functional investigation of cone opsin variants. *Hum Mutat*. 2014;35(11):1354–1362.
29. Sumaroka A, Cideciyan AV, Sheplock R, et al. Foveal therapy in blue cone monochromacy: predictions of visual potential from artificial intelligence. *Front Neurosci*. 2020;14:800.
30. Garafalo AV, Cideciyan AV, Héon E, et al. Progress in treating inherited retinal diseases: Early subretinal gene therapy clinical trials and candidates for future initiatives. *Prog Retin Eye Res*. 2020;77:100827.
31. Jacobson SG, Cideciyan AV, Ho AC, et al. Night vision restored in days after decades of congenital blindness. *iScience*. 2022;25(10):105274.
32. Farnsworth D. The Farnsworth-Munsell 100-hue and dichotomous tests for color vision. *J Opt Soc Am*. 1943;33(10):568–578.
33. Roth A. Le test 28 hue selon Farnsworth [Farnsworth's 28 hue test] [in French]. *Bull Soc Ophtalmol Fr*. 1966;66(2):231–238.
34. Amos JF, Piantanida TP. The Roth 28-hue test. *Am J Optom Physiol Opt*. 1997;54(3):171–177.
35. Birch J, Hamon L. Comments on the use of the standard pseudoisochromatic plates and the new color test of Lanthony. In: Colour Vision Deficiencies VII. *Doc Ophthalmol Proc Series*. 1984;39:221–226.
36. Erb C, Adler M, Stübiger N, Wohlrab M, Zrenner E, Thiel HJ. Colour vision in normal subjects tested by the colour arrangement test 'Roth 28-hue desaturated.' *Vis Res.* 1998;38(21):3467–3471.
37. Dain SJ. Clinical colour vision tests. *Clin Exp Optom.* 2004;87(4–5):276–293.
38. Hovis JK, Ramaswamy S, Anderson M. Repeatability indices for the Farnsworth D-15 test. *Vis Neurosci*. 2004;21(3):449–453.
39. O'Neill-Biba M, Sivaprasad S, Rodriguez-Carmona M, Wolf JE, Barbur JL. Loss of chromatic sensitivity in AMD and diabetes: a comparative study. *Ophthalmic Physiol Opt.* 2010;30(5):705–716.
40. Pedersen HR, Hagen LA, Landsend ECS, et al. Color vision in aniridia. *Invest Ophthalmol Vis Sci*. 2018;59(5):2142–2152.
41. Vemala R, Sivaprasad S, Barbur JL. Detection of early loss of color vision in age-related macular degeneration—with emphasis on drusen and reticular pseudodrusen. *Invest Ophthalmol Vis Sci*. 2017;58(6):BIO247–BIO254.
42. Abdel-Hay A, Sivaprasad S, Subramanian A, Barbur JL. Acuity and colour vision changes post intravitreal dexamethasone implant injection in patients with diabetic macular edema. *PLoS ONE*. 2018;13(6):e0199693.
43. Barbur JL, Rodriguez-Carmona M, Evans BEW. Color Vision Assessment-3: an efficient, two step, color assessment protocol. *Color Res Appl*. 2020;46:33–45.
44. Carroll J, Conway BR. Color vision. *Handb Clin Neurol*. 2021;178:131–153.
45. Luo X, Cideciyan AV, Iannaccone A, et al. Blue cone monochromacy: visual function and efficacy outcome measures for clinical trials. *PLoS One*. 2015;10(4):1–18.
46. Sumaroka A, Garafalo AV, Cideciyan AV, et al. Blue cone monochromacy caused by the C203R missense mutation or large deletion mutations. *Invest Ophthalmol Vis Sci*. 2018;59:5762–5772.
47. Barbur JL, Harlow J, Plant GT. Insights into the different exploits of colour in the visual cortex. *Proc Biol Sci*. 1994;258(1353):327–334.
48. Levitt H. Transformed up-down methods in psychoacoustics. *J Acoust Soc Am.* 1971;49(suppl 2):467+.
49. Birch J, Barbur JL, Harlow AJ. New method based on random luminance masking for measuring isochromatic zones using high resolution colour displays. *Ophthalmic Physiol Opt*. 1992;12(2):133–136.
50. Barbur JL, Rodriguez-Carmona M. Colour vision requirements in visually demanding occupations. *Br Med Bull*. 2017;122(1):51–77.
51. Vingrys AJ, King-Smith PE. A quantitative scoring technique for panel tests of color vision. *Invest Ophthalmol Vis Sci*. 1988;29(1):50–63.
52. Hartigan JA, Hartigan PM. The dip test of unimodality. *Ann Statist*. 1985;13(1):70–84, https://doi.org/10.1214/aos/1176346577.
53. Curcio CA, Sloan KR, Kalina RE, Hendrickson AE. Human photoreceptor topography. *J Comp Neurol*. 1990;292(4):497–523.
54. Curcio CA, Allen KA, Sloan KR, et al. Distribution and morphology of human cone photoreceptors stained with anti-blue opsin. *J Comp Neurol*. 1991;312(4):610–624.
55. Barbur JL, Konstantakopoulou E. Changes in color vision with decreasing light level: separating the effects of normal aging from disease. *J Opt Soc Am A Opt Image Sci Vis*. 2012;29(2):A27–A35.
56. Oliphant D, Hovis JK. Comparison of the D-15 and City University (second) color vision tests. *Vision Res*. 1998;38(21):3461–3465.

Downloaded from tvst.arvojournals.org on 03/01/2023

57. Weiss AH, Biersdorf WR. Blue cone monochromatism. *J Pediatr Ophthalmol Strabismus.* 1989; 26(5):218–223.
58. Ayyagari R, Kakuk LE, Bingham EL, et al. Spectrum of color gene deletions and phenotype in patients with blue cone monochromacy. *Hum Genet*. 2000;107(1):75–82.
59. Evans BEW, Rodriguez-Carmona M, Barbur JL. Color vision assessment 1: visual signals that affect the results of the Farnsworth D-15 test. *Color Res Appl*. 2021;46:7–20.
60. Atchison DA, Bowman KJ, Vingrys AJ. Quantitative scoring methods for D15 panel tests in the diagnosis of congenital color vision deficiencies. *Optom Vis Sci.* 1991;68(1):41–48.
61. Spivey BE. The X-linked recessive inheritance of atypical monochromatism. *Arch Ophthalmol*. 1965;74:327–333.
62. Pokorny J, Smith VC, Swartley R. Threshold measurements of spectral sensitivity in a blue monocone monochromat. *Invest Ophthalmol*. 1970;9(10):807–813.
63. Greenstein VC, Hood DC, Ritch R, Steinberger D, Carr RE. S (blue) cone pathway vulnerability in retinitis pigmentosa, diabetes and glaucoma. *Invest Ophthalmol Vis Sci*. 1989;30(8):1732–1737.
64. Hood DC, Greenstein VC. Blue (S) cone pathway vulnerability: a test of a fragile receptor hypothesis. *Appl Opt.* 1988;27(6):1025–1029.
65. Greenstein V, Sarter B, Hood D, Noble K, Carr R. Hue discrimination and S cone pathway sensitivity in early diabetic retinopathy. *Invest Ophthalmol Vis Sci.* 1990;31(6):1008–1014.
66. Remky A, Elsner AE. Blue on yellow perimetry with scanning laser ophthalmoscopy in patients with age related macular disease. *Br J Ophthalmol.* 2005;89(4):464–469.

Downloaded from tvst.arvojournals.org on 03/01/2023